of the individual runs. Let c_i be the normalization constant for run i. When there are only two domains to match, the matching involves finding a c such that

$$\sum_k w(1,2,k)^*[P_1(2,k) - c^*P_2(1,k)]^2 \rightarrow \text{minimum} \quad \text{(A1)}$$

where $w(1,2,k)$ is a weighting factor that should be designed to take into account the accuracy of the $P_1(2,k)$ and $P_2(1,k)$ values to ensure that the more accurate data will be dominant in determining the matching. In eq A1 and below, the sum over k is to be taken over all gridpoints that were sampled in both runs i and j. When there are more than two domains, then the scaling factors c_i should be determined by minimizing

$$\sum_{i=1}^{N_r} \sum_{j \in O(i)} \sum_k w(i,j,k)^*[c_i^*P_i(j,k) - c_jP_j(i,k)]^2 \quad \text{(A2)}$$

where $O(i)$ is the set of runs such that their domains overlap with the domain of i. Taking the partial derivative of (A2) with respect to each c_i, we obtain N_r linear equations:

$$c_i^* \sum_{j \in O(i)} \sum_k P_i(j,k)^2 - \sum_{j \in O(i)} c_j \sum_k P_i(j,k)^*P_j(i,k) = 0 \quad \text{(A3)}$$

Clearly, the equation system is homogeneous. As a result, it does not determine the solution fully. The remaining freedom in c_i, however, is needed at the end to determine the overall normalization factor that normalizes the global P to unity.

The necessity of solving a minimization problem introduces an added problem. There will be no unique value for the regions where two domains overlap. Furthermore, because of the many restrictions, there may even be significant breaks when the global P switches from one domain to another. This might necessitate the use of some smoothing, or restrict the use of the matching for more accurate distributions.

Registry No. AcAlaNHMe, 19701-83-8.

Metal–Metal Bonding and Antibonding Molecular Orbitals in Triangular Skeletons of the Type L_6M_3

Carlo Mealli

Contribution from the Istituto per lo Studio della Stereochimica ed Energetica dei Composti di Coordinazione, C.N.R., Via F. D. Guerrazzi 27, 50132 Florence, Italy. *Received July 23, 1984*

Abstract: The stabilization of triangular transition-metal frameworks of the type L_6M_3 is analyzed in terms of qualitative perturbation theory arguments and isolobal analogy concepts. Essentially each metal of the M_3 triangle is required to have two orbitals, one each of σ and π symmetry, which nest as three bonding (two tangential and one radial) and three antibonding (one tangential and two radial) MOs. Six electrons in the former and none in the latter set confer maximum stability to the system by analogy to the known electronic features of cyclopropane. The required energy level ordering is not attainable with models having three terminal L_2M fragments, unless supported by the presence of other coligands. The reason for this failure is that each L_2M fragment has a σ hybrid which is too destabilized, hence the intermetal radial bonding combination of these hybrids cannot descend below the tangential antibonding combination of π orbitals. Conversely, L_6M_3 clusters are stabilized when three of the six ligands function as bridges between metals. This structure, referred to as "unsupported-bridged", may be considered as formed by three planar L_3M fragments, and this allows the correct order of the direct bonding and antibonding M–M orbitals. Strategies for the extraction of the latter from the group of M–L bonding–antibonding orbitals are indicated in the presence of either π-acceptor or π-donor bridging ligands. In some instances one of the three M–M antibonding orbitals is also low enough in energy to be populated. Usually this lowers the calculated M–M bond order which is consistent with the experimental long M–M distances. Examples of "supported-unbridged" geometry are also known. The supporting ligands are capping one or both faces of the M_3 triangle formed by three terminal L_2M groupings. In other cases bridging hydrogen atoms provide the required support. It is shown that the main action of the supporting ligands is that of enriching the sp character of a particular radial bonding combination of metal d orbitals which thus stabilizes below a competing tangential antibonding M–M combination. The present analysis gives new weight to the contribution of metal d orbitals in the M_3 bonding network and allows the identification of the corresponding MOs.

It has been proposed that D_{3h} trinuclear metal clusters are the inorganic equivalent of cyclopropane.[1] The bonding network of cyclopropane can be constructed by means of two localized hybrids at each carbon atom containing one electron each, as shown in **1**.[2] In terms of MO theory one σ and one π orbital at each center concur to form three radial (a'_1 and e'_r) and three tangential (a'_2 and e'_t) combinations. Three C–C single bonds are then formed since the bonding combinations a'_1 and e'_t are fully occupied, as shown in **2**.

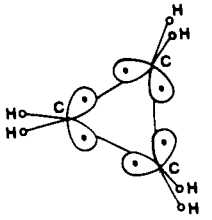

1

Similar schemes may be constructed for triangular metal clusters provided that each metal fragment has suitable σ and π orbitals. There is sufficient evidence that the L_6M_3 skeleton can exist by itself only if three L ligands function as bridges between two metals in what can be referred to as "unsupported-bridged" geometry. In other cases the required bonding–antibonding arrangement of the levels is attained because of the presence of other coligands, either capping one or both faces of the M_3 triangle or bridging three L_2M fragments approximately in the molecular

(1) Hoffmann, R. *Angew. Chem., Int. Ed. Engl.* **1982**, *21*, 711–724.

(2) (a) Jorgensen, W. L.; Salem, L. "The Organic Chemist's Book of Orbitals"; Academic Press: New York, 1973; pp 19–23. (b) Hoffmann, R. "Special Lectures at the 23rd International Congress of Pure Applied Chemistry"; Butterworths; London, 1971; Vol. 1, p 157.

0002-7863/85/1507-2245$01.50/0

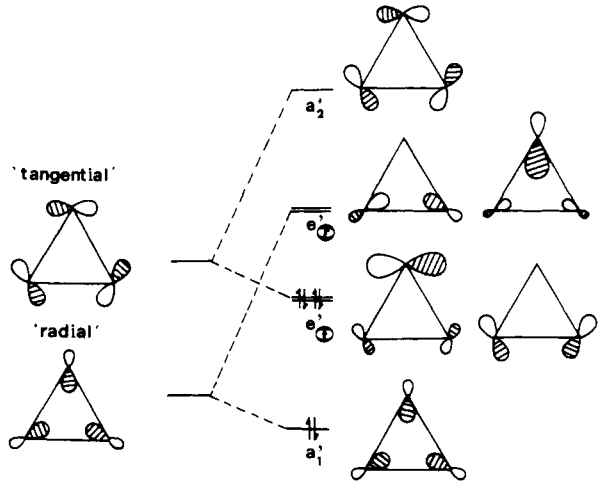

2

plane. The latter will be called "supported-unbridged" coordination.

Quantitative results of MO calculations are already abundant and sophisticated for triangular clusters;[3] the present paper uses qualitative perturbation theory arguments for the interpretation of the bonding, geometry, and stability in the restricted class of L_6M_3 species.

Discussion

"Unsupported-Bridged" Coordination. Isolobal analogy, a powerful interpretational tool,[1,4] can predict the assembly of three d^{10} L_2M fragments, isolobal with CH_2, to originate a latitudinal conformer of type **3**. In contrast, direct evidence of such an "unsupported-unbridged" structure is missing.

3

The MO pattern **4** has many analogies with **2** irrespective of the reversed order of the σ and π orbitals at each L_2M building block[5] and of their relatively higher energy gap. An a'_1 below an a'_2 level, as in **4**, is suggestive of the stabilization of 42-e species, as noticed by Evans and Mingos.[3e] A reversed ordering would

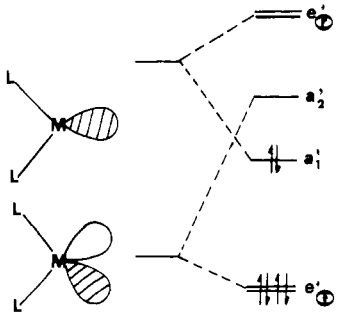

4

induce destabilization since all the bonding and antibonding combinations of metal π orbitals would then be filled. The latter result was implicit in the arguments of Dedieu and Hoffmann,[3b] who based their analysis on the L_4M_2–L_2M fragmentation of the cluster. All of these authors also seem to agree on the fact that a 90° rotation of the L_2M planes, to generate a longitudinal conformer **5**, would definitely not be stabilizing for a 42-e species. In this case the tangential combinations of the metal π orbitals, namely e'_t and a'_2, would be formed with pure d orbitals rather than with d–p hybrids.[5] The minor destabilization of a'_2, on account of poorer overlap, energetically favors the longitudinal over the latitudinal conformer[3e] but still does not ensure the favorable level ordering **4**.

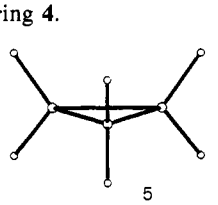

5

The relative order of the a'_1 and a'_2 levels critically depends on the size of the M_3 triangle. Figure 1 shows the energies of the cluster frontier orbitals e'_t, a'_1, and a'_2 plotted as a function of the "implosion" parameter r which governs the assembly of three $(CO)_2Pt$ fragments along a D_{3h} pathway. Only for short values

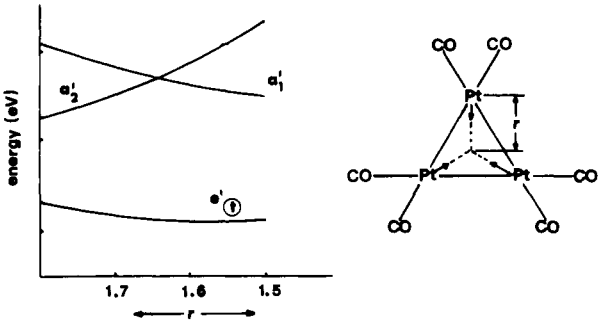

Figure 1. Evolution of frontier orbitals as a function of the "implosion" parameter r which governs the assembly of three $(CO)_2Pt$ fragments along a D_{3h} pathway. An r value of 1.5 Å corresponds to a Pt–Pt separation of ca. 2.6 Å.

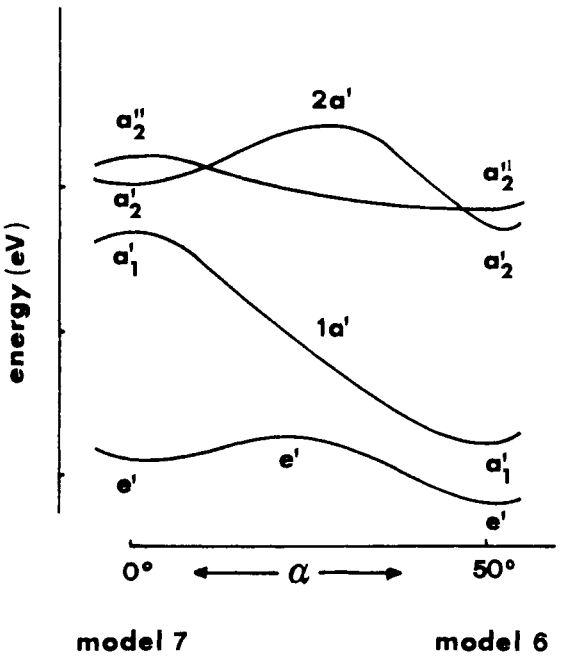

Figure 2. Evolution of the frontier orbitals of $Pt_3(CO)_6$ as a function of the α rotations which interconvert terminal and bridged geometries. The MO a''_2 is a combination of CO π^* and metal p_z orbitals and is schematically shown in **13** for the model **6**.

(3) (a) Ruff, J. K.; White, R. P., Jr.; Dahl, L. F. *J. Am. Chem. Soc.* **1971**, *93*, 2159–2176. (b) Dedieu, A.; Hoffmann, R. *J. Am. Chem. soc.* **1978**, *100*, 2074–2079. (c) Lauher, J. W. *J. Am. Chem. Soc.* **1978**, *100*, 5305–5315. (d) Evans, J. *J. Chem. Soc., Dalton Trans.* **1980**, 1005–1011. (e) Evans, G. D.; Mingos, M. P. *J. Organomet. Chem.* **1982**, *240*, 321–327. (f) Rives, A. B.; Xiao-Zeng, Y.; Fenske, R. F. *Inorg. Chem.* **1982**, *21*, 2286–2294. (g) Manning, M. C.; Trogler, W. C. *Coord. Chem. Rev.* **1981**, *38*, 89–138 and references therein. (h) Schilling, B. E. R.; Hoffmann, R. *J. Am. Chem. Soc.* **1979**, *101*, 3456–3467. (i) Pinhas, A. R.; Albright, T. A.; Hofmann, P.; Hoffmann, R. *Helv. Chim. Acta* **1980**, *63*, 29–49. (j) Cotton, F. A.; Haas, T. E. *Inorg. Chem.* **1964**, *3*, 10–17. (k) Bursten, B. E.; Cotton, F. A.; Green, J. C.; Seddon, E. A.; Stanley, G. G. *J. Am. Chem. Soc.* **1980**, *102*, 955–968. (l) Tyler, D. R.; Levenson, R. A.; Gray, H. B. *J. Am. Chem. Soc.* **1978**, *100*, 7888–7893. (m) Exhaustive reference lists are also found in "Transition Metal Clusters"; Johnson, B. F. G., Ed.; John Wiley: New York, 1980.

(4) Elian, M.; Chen, M. M.-L.; Mingos, D. M. P.; Hoffmann, R. *Inorg. Chem.* **1976**, *15*, 1148–1155.

(5) Albright, T. A. *Tetrahedron* **1982**, *38*, 1339–1388 and references therein.

of r (at least corresponding to Pt–Pt separations of ca. 2.8 Å) does a'_1 become lower in energy than a'_2. Also notice that, for 42-e species, this D_{3h} assembly pathway is symmetry forbidden on account of a HOMO–LUMO crossing (a'_1 and a'_2, respectively).

Although the most classical example of unsupported L_6M_3 species is the 44-e dianion $[Pt_3(CO)_6]^{2-}$ (I), the building block of the stacked polymers $[Pt_3(CO)_6]_n^{2-}$ (II),[6] the crystal structure of I has never been investigated. However, crystallographic data are available for closely related 42-e clusters such as $[Pt_3(t\text{-BuCN})_6]$ (III),[7] and $(Pt_6(CO)_3[(P(C_6H_{11})_3]_3)$ (IV).[8] In these structures, schematically shown in **6**, the Pt–Pt linkages[9] of ca. 2.65 Å are bridged by CO or t-BuCN π-acceptor groupings. EHMO calculations show that **6** is a far more stable model than **7**. The very large ΔE value (>100 kcal/mol for L′ = L = CO)

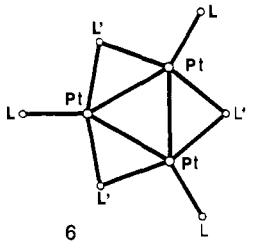

6

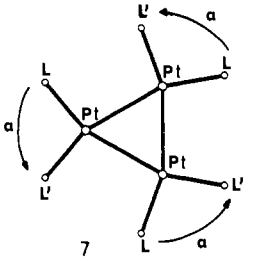

7

confirms the experimental NMR result that bridging and terminal carbonyls retain their identity.[10] A great part of the stabilization in the bridged structure comes from the steep decrease in energy (ca. 2 eV) of the HOMO (a'_1). This is clearly seen in Figure 2 where the MO levels are plotted as a function of α, the parameter of the simultaneous rotations of the L_2M units about axes orthogonal to the molecular plane and passing through the metals. For the particular geometry chosen (Pt–Pt = 2.7 Å, Pt–CO = 2.1 Å), α rotations of 50° interconvert **6** and **7** through a C_{3h} pathway.[11] Along the pathway the a'_1 and a'_2 levels become of equal symmetry, a′, and avoid a crossing irrespective of their relative initial order.

Why is the a'_1 level stabilized so much in the bridged structure? Does it still have the significance of an intermetal radial bonding orbitals which is needed for the analogy with the cyclopropane case? Actually, on account of the highly delocalized electronic structure through the bridges, it is difficult to identify, at each metal, the basic σ and π hybrids suited for constructing a pattern of type **2** or **4**.

In this respect also the FMO calculations[12] do not offer immediate help because cluster **6** cannot be sectioned into three equal metal fragments. Only conceptually can one split into halves the bridging ligands and, if the bridges are capable of donating a σ lone pair to each adjacent metal, assemble the cluster from three planar L_3M fragments as in **8**. Ideally, the latter fragments derive from square-planar complexes after the removal of one ligand and the opening of two L–M–L angles from 90° to 100°. The latter deformation little affects the two σ and π frontier orbitals of L_3M (**9** and **10**) needed for the construction of scheme **4**. At variance with the corresponding σ orbital of the L_2M fragment, **9** has more d character, and hence is located at significantly lower energy. As a consequence, the a'_1 radial combination is also stabilized.

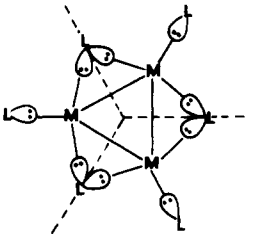

8

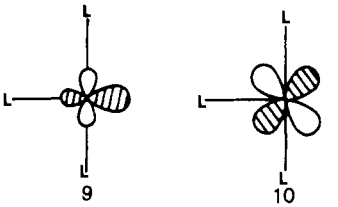

9 10

Obviously, the idea of a L_6M_3 cluster as assembled from three L_3M units is more acceptable if the bridging ligands have π-donor character (e.g., halides or phosphido groups) since two localized lone pairs, to be donated to the metals, can be constructed by using filled σ and π orbitals. Compounds such as $[Pt_3(PPh_3)_3(PPh_2)_2Ph]$ (V)[13] or $[Pd_3Cl(PPh_2)_2(PEt_3)_3]^+$ (VI)[14] belong to this category although in V one of the Pt–Pt distances is nonbonding and the Pt_3 triangle has an isosceles shape. Representations of V and VI are shown in **11** and **12**, respectively.

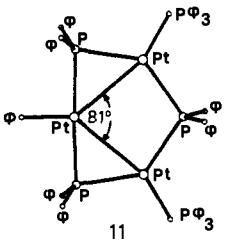

11

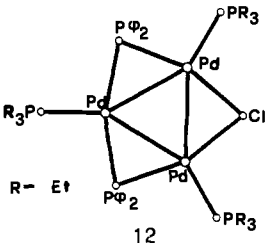

12

By contrast, carbon monoxide molecules are usually considered 2-e donors at most, and it is more difficult to recognize them as capable of donating two lone pairs to the metals. The following MO analysis helps to clarify the role of the bridging phosphido and carbonyl groups, respectively.

For quantitative calculations model **6** was sectioned into the fragments L_3M_3 and L'_3 (where L'_3 is the assembly of the three bridging ligands). Unfortunately, this type of FMO analysis mainly focuses attention on the interactions between the metals and the bridging ligands, rather than on the direct metal–metal interactions. Hopefully these M–M interactions can be revealed through indirect arguments. Figure 3 compares the simplified diagrams for interactions between the $(CO)_3Pt_3$ core and two different L'_3 systems, namely $(PH_2)_3$, at the left, and $(CO)_3$, at the right.

Only the interactions between "in-plane" orbitals are interesting for the formation of six Pt–L′ and three Pt–Pt bonds—thus the remaining orbitals are not shown with the single exception (in Figure 3d) of a''_2, **13**, which is a combination of carbonyl π^* orbitals with some metal p_z character involved.[15]

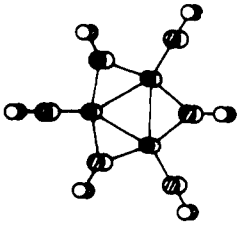

13

(6) Longoni, G.; Chini, P. *J. Am. Chem. Soc.* **1976**, *98*, 7225–7231.
(7) Green. M.; Howard, J. A. K.; Murray, M.; Spencer, J. L.; Stone, F. G. A. *J. Chem. Soc., Dalton Trans.* **1977**, 1509–1514.
(8) Albinati, A. *Inorg. Chim. Acta* **1977**, *22*, L31–L32.
(9) Besides the structural data, NMR studies confirm the existance of Pt–Pt bonds in **4**. See: Moor, A.; Pregosin, P. S.; Venanzi, L. M. *Inorg. Chi. Acta* **1981**, *48*, 153–157.
(10) Brown, C.; Heaton, B. T.; Chini, P.; Fumagalli, A.; Longoni, G. *Chem. Commun.* **1977**, 309.
(11) For L = CO three of the six Pt–C–O vectors must be progressively bent up to a maximum of 40° during the rotations α. Thus for any 10° of the latter rotation the Pt–C–O angle is bent 8°.
(12) The theoretical basis of the fragment orbital analysis are found in the following: Fujimoto, H.; Hoffmann, R. *J. Phys. Chem.* **1974**, *78*, 1167. Hoffmann, R.; Swenson, J. R.; Wan, C.-C. *J. Am. Chem. Soc.* **1973**, *95*, 7644–7650.
(13) Taylor, N. J.; Chieh, P.; Carty, A. J. *Chem. Commun.* **1975**, 448–449.
(14) Bushnell, G. W.; Dixon, K. R.; Moroney, P. M.; Rattray, A. D.; Wan, C. *Chem. Commun.* **1977**, 709–710.

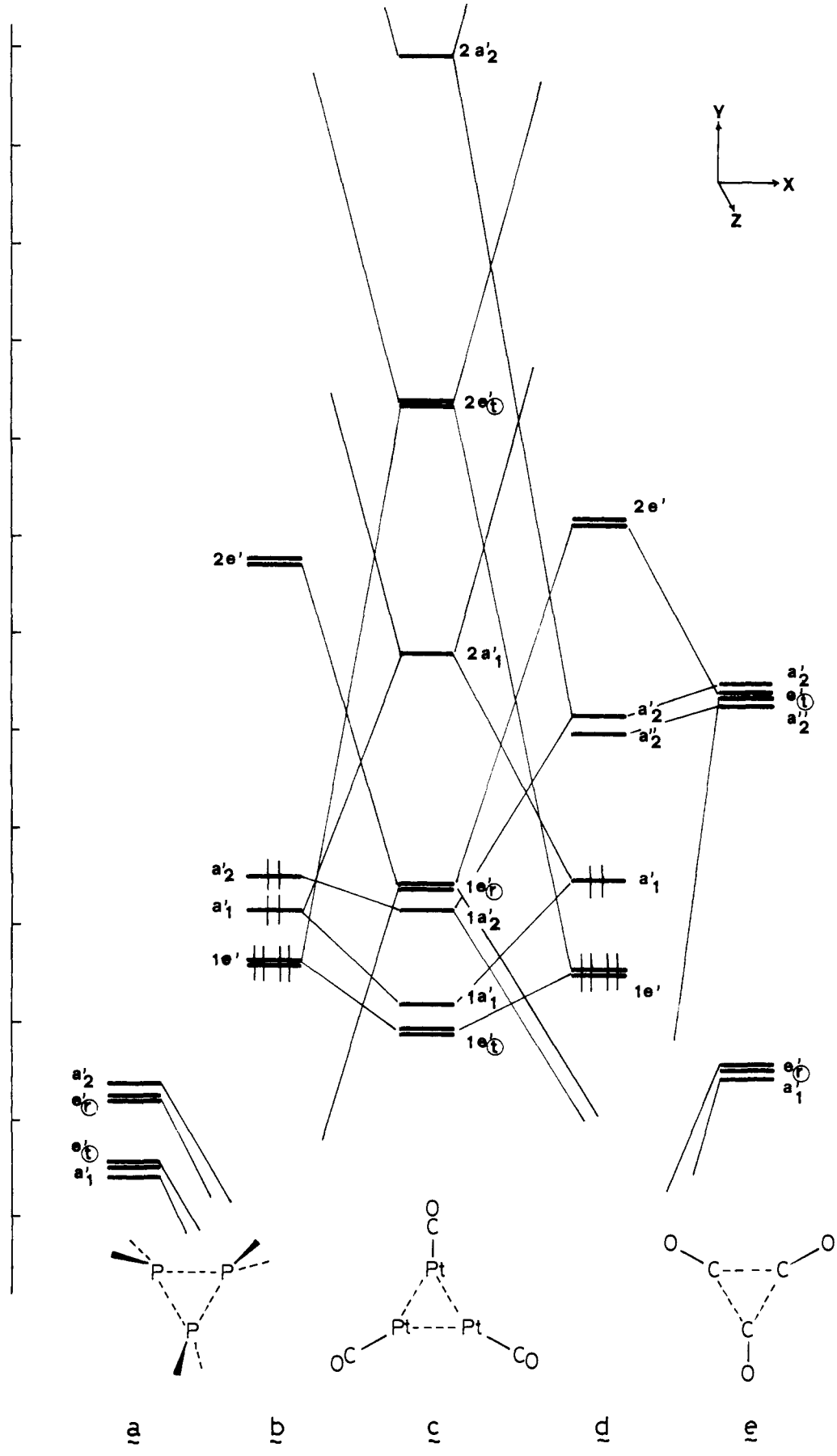

Figure 3. Interactions between the FMOs of a $Pt_3(CO)_3$ grouping (c) and those of three bridging ligands having π-donor (a) or π-acceptor (e) capabilities.

Figure 3c contains two distinct groups of metal levels, each one consisting of the D_{3h} combinations of σ (radial) and π (tangential) orbitals, in analogy with patterns **2** or **4**. These are the following: (i) the levels having metal d character, $1e'_t$, $1a'_1$, $1a'_2$, $1e'_r$, to be considered all populated for d^{10} species (for the particular choice of the axes these FMOs are combinations of xy and x^2-y^2 d orbitals); and (ii) the levels having p or sp metal character (s, p_x, p_y), $2a'_1$, $2e'_t$, $2a'_2$, $2e'_r$ (the latter $2e'_r$ set, being too high in energy, is not shown).

Similarly a set of six (three radial and three tangential) orbitals of a'_1, e'_t, e'_r, a'_2 symmetry can be constructed with appropriate "in-plane" L'_3 orbitals. Figure 3, a and e, reports this set for π-donor and π-acceptor bridging ligands, respectively. The orbitals in Figure 3a are compact and low in energy. In Figure 3e the radial combinations, a'_1 and e'_r, are separated from the tangential ones, e'_t and a'_2, since the latter are formed with high-lying carbonyl π^* orbitals.

The positive overlap populations[16] between selected fragment orbitals of Figure 3, a and c, are clearly indicative of six M–L bonding interactions. These are $\langle a'_1|2a'_1\rangle$, $\langle e'_t|1e'_r\rangle$, $\langle e'_r|2e'_t\rangle$, and $\langle a'_2|2a'_2\rangle$. Notice that radial e' sets of the metals interact with tangential e' sets of the ligands and vice versa. As an example, **14** shows the ligand–metal interaction $\langle e'_r|2e'_t\rangle$.

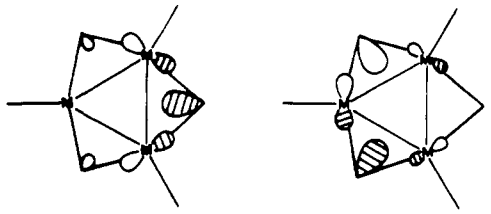

14

Ultimately six bonding and six antibonding Pt–PH_2 levels are formed from the 18 fragment orbitals under consideration. The two groups are well separated in energy and, of these, only 2e' appears in Figure 3b. The orbitals 1e', a'_1, a'_2, together with the very high lying metal sp radial setting 3e', not shown in Figure 3b, may be proposed as the three bonding and three antibonding Pt–Pt combinations. Importantly, the $1e'_t$ and, to a much larger extent, the $1a'_1$ combinations of metal d orbitals (see Figure 3c), on account of a second-order perturbation,[17] undergo an intrafragment hybridization with the higher metal p and sp combinations of equal symmetry.[18] Scheme **15** shows how the rehybridization occurs. The presence of more diffuse orbitals is largely responsible

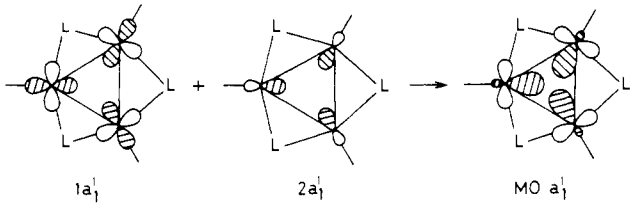

15

for the direct metal–metal bonding interactions, as is also emphasized by other workers.[3b,e,f] However, the present analysis gives new weight to the contribution of d orbitals in M_3 bonding and also allows the identification of the corresponding MOs. It is also interesting that the $1a'_2$ M–M antibonding combination remains at low energy, practically unhybridized, with the important consequence that filling it with two electrons weakens but does not destroy the metal–metal bond. This point will receive further attention later (vide infra).

The MO levels of $(CO)_6Pt_3$ are shown as Figure 3d. Again there is a total of 12 M–CO bonding and antibonding combinations formed by the ligand and metal species respectively: $\langle a'_1|2a'_1\rangle$, $\langle e'_r|1e'_t\rangle$, $\langle a'_2|1a'_2\rangle$, and $\langle e'_t|1e'_r\rangle$. At variance with the previous case involving PH_2 bridges, the M_3 grouping uses the $1a'_2$ rather than the $2a'_2$ set to make one bonding interaction with the ligands. In effect, metal electron density is transferred from 1a' (and from $1e'_r$ as well) into the higher, empty, carbonyl π^* combinations. Thus the a'_2 level, shown in Figure 3d, definitely has a metal–ligand rather than a metal–metal antibonding character. Also, the energy of a'_2, in spite of the stabilizing mixing with the metal $2a'_2$ level, is quite high for it to be populated. For this reason L_6M_3 systems with π-acceptor bridges prefer a 42-e configuration.

Note that three of the six M–L' bonding interactions originate from the donation of metal electrons into empty L'_3 orbitals. Alternatively, CO^{2-} anions may be considered to be analogous with bridging PH_2^- groups, each capable of donating two electron pairs to the metals. In support of this viewpoint is the fact that in compound **3** the *t*-BuCN groups are linear in terminal, but bent in bridging, positions. This agrees with the known rules which rationalize the bending of HAB (or RAB) molecules with an increasing number of valence electrons.[19] Even though CO^{2-} anions sound unfamiliar, the point to be made is that electron pairs are shared between carbonyl π^* and suitable metal orbitals. Importantly, the primary stability of the system is provided by these first-order interactions between the bridging ligands and the metal framework. In addition, the information gathered is also valuable for learning how to separate direct M–M from M–L interactions.

Another example is also illuminating. The apparently complicated hexanuclear clusters $[Fe_2Pt_3(CO)_{15}]^n$ (n = 1–, 2–) (VII),[20] schematically shown in **16**, may be described in terms of model **6**. Three $(CO)_4Fe$ fragments represent the bridges between three (CO)–Pt fragments. A d^8 $(CO)_4Fe$ fragment with geometry **17**

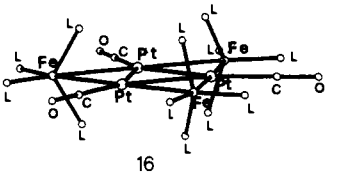

16

is characterized by a σ, **18**, and a π orbital, **19**, which carry a total of two electrons, analogous to the CH_2 fragment, or to CO or CNR ligands.

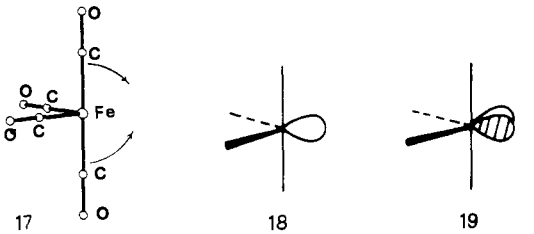

17 18 19

By contrast, in VII the axial (O)C–Fe–C(O) vector is significantly bent in the direction indicated in **17**, namely toward a tetrahedron which is more consistent with a d^{10} electronic configuration of the metal. In this case both the σ and π orbitals, derived from **18** and **19**, would be filled and would be able to form two localized hybrids acting as lone pairs donated to the Pt atoms.

M–M distances of 2.6–2.7 Å are usually observed in 42-e "unsupported-bridged" clusters. The higher limit was found in $[Pt_3(SO_2)_3(PPh_3)_3]$ (VIII).[21,22] The previous considerations, based

(15) This MO was recognized as the HOMO in I.[3c,d] Due to its out-of-plane directional properties it is likely responsible for the formation of the stacked polymers II.

(16) Values in the range 0.16–0.54 are calculated for a 44e configuration such as that found in compounds V and VI.

(17) Elian, M.; Hoffmann, R. *Inorg. Chem.* **1975**, *14*, 1058–1076. Libit, L.; Hoffmann, R. *J. Am. Chem. Soc.* **1974**, *96*, 1370–1383.

(18) The composition of a'_1 in d has 27% character of metal $2a'_1$ and 70% of $1a'_1$ and other lower orbitals; the contribution of $(PH_2)_3$ ligands is only 3%. Conversely, the composition of the 1e' set is 5% of metal $2e'_t$, 64% of $1e'_t$ (plus 15% of lower orbitals) and finally 6% of bridging $(PH_2)_3$ e' set.

(19) Gimarc, B. M. "Molecular Structure and Bonding"; Academic Press: New York, 1979; p 113–116 and 153–165.

(20) Longoni, G.; Manassero, M.; Sansoni, M. *J. Am. Chem. Soc.* **1980**, *102*, 7974–7976.

(21) Moody, D. C.; Ryan, R. R. *Inorg. Chem.* **1977**, *16*, 1052–1055.

on the assumption that each metal receives a lone pair from each ligand (terminal or bridging), imply a d^{14} total electron count at each L_3M unit. Consequently three M–M single bonds must be operative to attain a saturated 16-e configuration at each planarly coordinated metal. This is schematically shown in **20**.

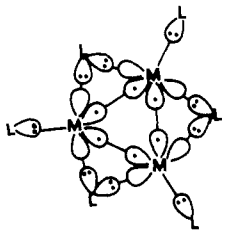

20

In 44-e compounds containing π-donor bridging ligands, there is a populated metal a'_2 level at sufficiently low energy so that it is not involved in metal–ligand antibonding. In this case the M–M antibonding nature of the orbital significantly lengthens the M–M separation of ca. 2.9 Å in VI. The MO arguments (in which three bonding orbitals and one antibonding orbital are occupied) and the fact that the L_3M unit has a formal electron count of 14.67 are suggestive that the M–M bond order is $^2/_3$. In compound V one Pt–Pt separation is longer than the bonding distance and the cluster has a lower C_{2v} symmetry. By contrast, a series of MO calculations show that the minimum of the total energy is found at D_{3h} symmetry (there are about 25 kcal/mol of destabilization in opening one Pt–Pt–Pt angle from 60° to 85°). In fact, the energy gained by partially reducing the antibonding of the a'_2 level does not compensate the energy lost by the Pt_3 bonding orbitals namely a'_1 and $1e'_1$. On the other hand, steric arguments are certainly important because the long Pt–Pt distance occurs where the bulky diphenylphosphido group bridges two $Pt(PPh_3)$ fragments (see **11**).

Figure 3d shows a small energy gap between a'_2 and a''_2 levels, which are the candidates for the HOMO in 44-e species having π-acceptor bridging ligands such as I or VII. The structure of I is not known. Although the propensity of this compound to polymerize in a direction perpendicular to the molecular plane seems to favor a''_2 as the HOMO, it may be possible that this reactivity is promoted by excited states or Jahn–Teller second-order effects. On the other hand, the increase of the Pt–Pt separation from 2.65 to 2.75 Å in going from the monoanionic to the dianionic conformer of VII is suggestive of the antibonding a'_2 nature of the HOMO. Confirmation of this is provided by EHMO calculations carried out for the simplified model **16**, with L = H and the molecular charges properly adjusted. The HOMO is calculated to have a percentage of iron character almost twice that of platinum, and this accounts for the fact that the Pt–Pt distances are not dramatically affected by the different electron population.

"Supported-Unbridged" Coordination. Up to this point only the electronic requirements for the stability of the "unsupported-bridged" L_6M_3 clusters were analyzed. Returning to the latitudinal conformer **3**, this is found as the skeleton in the compound $[Pd_3(\mu^3\text{-}CO)(\mu\text{-}Ph_2PCH_2PPh_2)_3]^{2+}$ (IX),[24] illustrated in **21**, where the presence of a capping CO molecule clearly has a stabilizing effect. In compound $[(COD)_3Pt_3(SnCl_3)_2]$ (X),[25] **22**, the skeleton is supported by two capping $SnCl_3$ groups, whereas in the isoelectronic $[Pt_3H_6(P\text{-}t\text{-}Bu_3)_3]$ (XI)[26] **23**, and $[Rh_3(P(OCH_3)_3)_6H_3]$ (XII),[27] three bridging hydrogen atoms play an analogous supportive role.

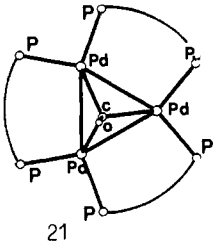

21

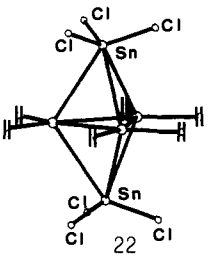

22

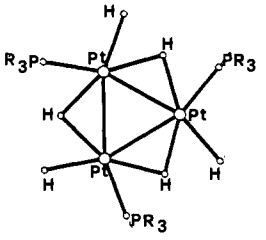

23

The electronic features of these "supported-unbridged" compounds may be tentatively described from an unique viewpoint. The idea is still that of separating the metal orbitals engaged in bonding with the supporting ligands from those metal orbitals which eventually participate in the formation of direct M–M bonds. Figure 4 shows parallel diagrams for the interaction of a $(CO)_6Pt_3$ fragment, of type **7**, with one CO or two $SnCl_3$ capping units, respectively. The $(CO)_6Pt_3$ levels, in Figure 4c, are characterized by the high energy of the radial $2a'_1$ MO. The latter is the same as the a'_1 orbital in **4** and in Figure 1. Consequently, there is a low probability of populating this level, even if it lies below the tangential a'_2 MO when the M–M distances are reasonably short. The capping ligand(s) removes $2a'_1$ from the LUMO area, due to a three-orbital interaction. The three-orbital interaction occurs because on the appropriate side of the capping ligand(s) there is a lone pair(s) which points toward the center of the M_3 triangle. On the appropriate side of the metals, the radial combination of sp hybrids ($2a'_1$) as well as a set of pure orbitals ($1a'_1$) are involved. The latter $1a'_1$ set is shown in **24**

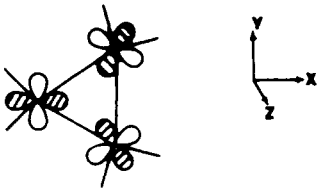

24

where, for the given system of axes, the left-most metal atom participates with the x^2-y^2 orbital.

Whatever the relative order of the three metal and ligand combinations, bonding, nonbonding, and antibonding levels occur. It is significant that in the nonbonding levels (a_1 and a'_1 in Figure 4, b and d, respectively) an intrafragment metal d–s–p rehybridization (comparable with that in **15**) allows the possibility of direct metal–metal bonding interactions. Conversely, the FMO a'_2 (M–M antibonding) is not affected by the presence of the supporting ligands and remains unperturbed at high energy. The combination e'_t, which, with reference to pattern **4**, is the other

(22) In spite of the somewhat long Pt–Pt distances VIII may be classified as a cluster with π-acceptor bridges. In fact SO_2 molecules have an in-plane sp^2 lone pair and an orthogonal sulfur p_z empty orbital which is part of a $\pi_\perp^*$ SO_2MO.[21] The 2.78 Å Pt–Pt vector bridged by SO_2 in $[Pt_3(\mu\text{-}PH)(\mu\text{-}PH_2)(\mu\text{-}SO_2)(PPh_3)_3]$[23] does not properly represent an exception because it is inserted in a Pt_3 triangle with three bridges that have different π capabilities. In such a case the M–M separations cannot be evaluated individually but only in global through an ad hoc MO calculation. The interpretation of the latter is, however, predictably difficult on account of the low symmetry of the molecule.

(23) Evans, D. G.; Hughes, G. R.; Mingos, D. M. *Chem. Commun.* **1980**, 1255–1257.

(24) Manojlovic-Muir, L.; Muir, K. W.; Lloyd, B. R.; Puddephatt, R. J. *Chem. Commun.* **1983**, 1336–1337.

(25) Guggenberger, L. J. *Chem. Commun.* **1968** 512–513.

(26) Frost, P. W.; Howard, J. A. K.; Spencer, J. L.; Turner, D. G. *Chem. Commun.* **1981**, 1104–1105.

(27) Brown, R. K.; Williams, J. M.; Sivak, A. J.; Muetterties, E. L. *Inorg. Chem.* **1980**, *19*, 370–374.

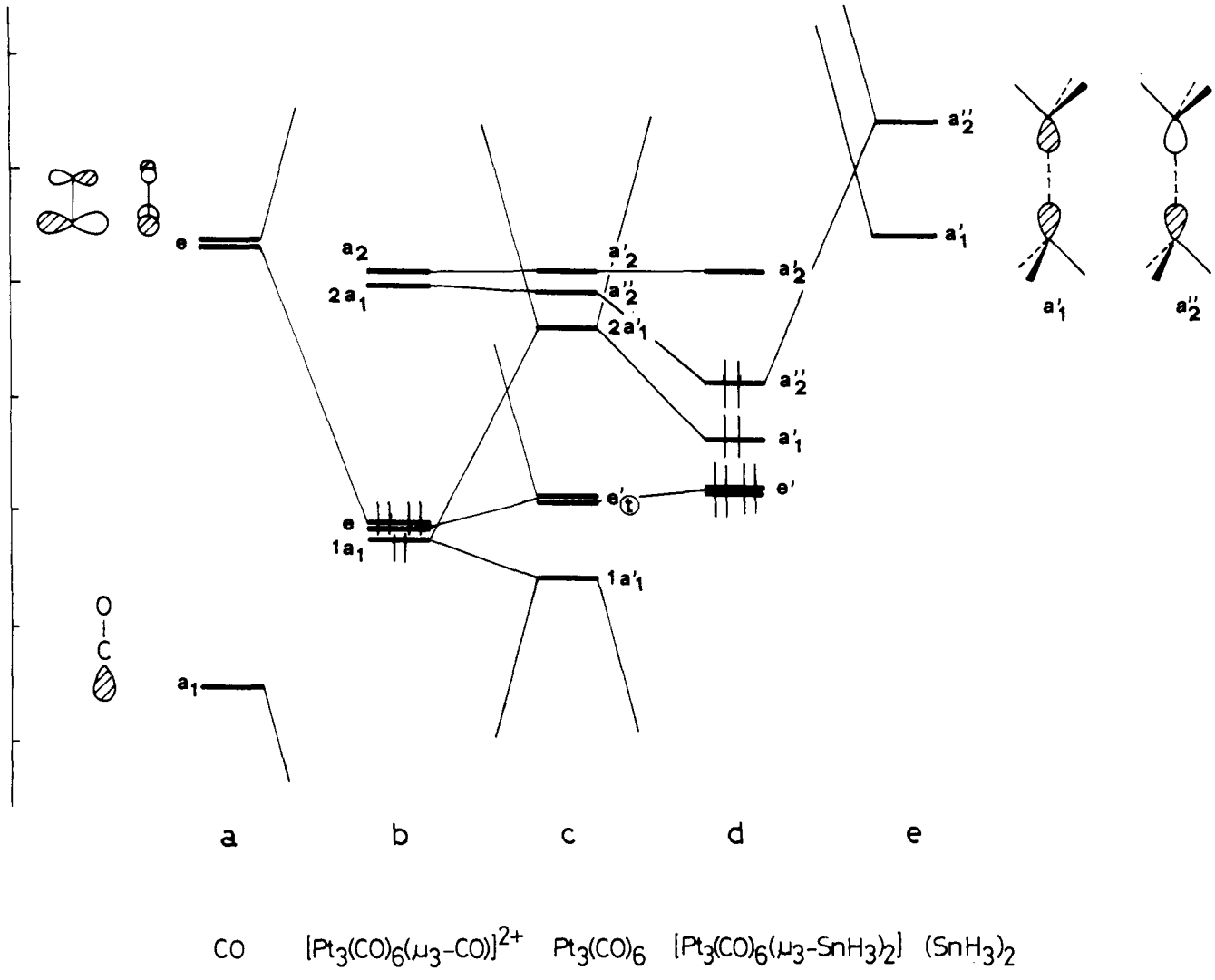

Figure 4. Interactions between the FMOs of a $Pt_3(CO)_6$ cluster with geometry **7** (c) and those of a capping CO molecule (a) or two capping $SnCl_3$ groups (e).

important M–M bonding level, interacts slightly with the carbonyl π^* e set (Figure 4b) thus reinforcing the M_3–CO linkage through a partial transfer of M–M bonding electrons into CO. By contrast e'_t remains unperturbed in Figure 4d because the $SnCl_3$ groups lack proper π orbitals. Thus for the above reasons the M–M bonds are expected to be slightly stronger in X than in IX. The small difference is in the proper direction [2.60 (1) vs. 2.58 (1) Å], but it is not significant even in view of the different nature of the metals (Pt or Pd). Notice, however, that in both compounds there is a significant shrinkage (~0.05 Å) with respect to clusters with "unsupported-bridged" geometry. The overlap argument is important here because the bonding tangential e'_t set is formed by almost pure d orbitals in the "unsupported-bridged" case (see **10**), whereas, in the present cases, the terminal L_2M groups participate to the bonding e'_t interactions with the well-hybridized π orbitals, shown in **4**.

As a final remark the MO analysis indicates only two bonding interactions (of a'_1 and a''_2 type) between the FMO, Figure 4, c and e. In the a''_2 level, an out-of-plane L_6M_3 orbital of composition similar to **13** combines with the proper combination of $SnCl_3$ σ orbitals. In summary, two delocalized Sn–Pt_3 linkages, rather than six distinct Pt–Sn bonds, can be envisaged at most. This agrees well with the long Sn–Pt separations of ca. 2.8 Å observed in X.

Compounds XI and XII are analyzed by the following criteria. The model adopted is $[Pt_3(CO)_6H_3]^{3+}$ which has D_{3h} symmetry so that the three bridging H atoms lie coplanar with the L_6M_3 skeleton. This is close to the geometry intuitively seen in XI,[26] although in XII the planar geometry is greatly distorted.[28] The interaction diagram of Figure 5 illustrates the role of the bridging hydrogen atoms. Combinations a'_1 and e′ are formed with the H_3 orbitals in D_{3h} symmetry. The former level participates in a bonding–antibonding interaction with the metal $2a'_1$ combination of sp hybrids, but again the important effect is that, because of the presence of the H ligands, the metal $1a'_1$ level takes some of the sp character of $2a'_1$ with consequent benefits for the overlap and energetics of the M–M bonding radial combination. The other H_3 level, e′, involves the metal e'_t combination in a bonding–antibonding interaction. Thus the MO e′, at the center of Figure 5, has acquired M–H bonding character at the expense of M–M bonding character. This agrees well with the lengthening of the Pt–Pt distances up to 2.80 (3) Å in XI and XII. It is also worth noting that rotations of the L_2M fragments about the M–cluster centroid vectors, as observed in XII, do not affect the radial combinations of σ orbitals which seem to be the cementing force in the clusters. In any event, the metal π orbitals (originally e'_t) lose their direct M–M bonding character, and hence they may adapt to seek a maximum interaction with the out-of-plane H_3 e set.

(28) The distortion is very likely attributable to the high steric demands of terminal phosphines as has already been suggested by others.[3e] It is remarkable that short H··H contacts cannot be avoided when constructing simple models having all terminal PH_3 molecules with Pt–Pt separations of 2.80 Å or less. As a consequence it is improbable that conformers of type **7** may be formed with any monophosphine ligand unless it is severely distorted. Bidentate phosphines such as diphos do not encounter the same obstacle, as shown by the formation of VIII. Also, to avoid the problem of the steric repulsion, terminal CO ligands were usually used in the present MO study.

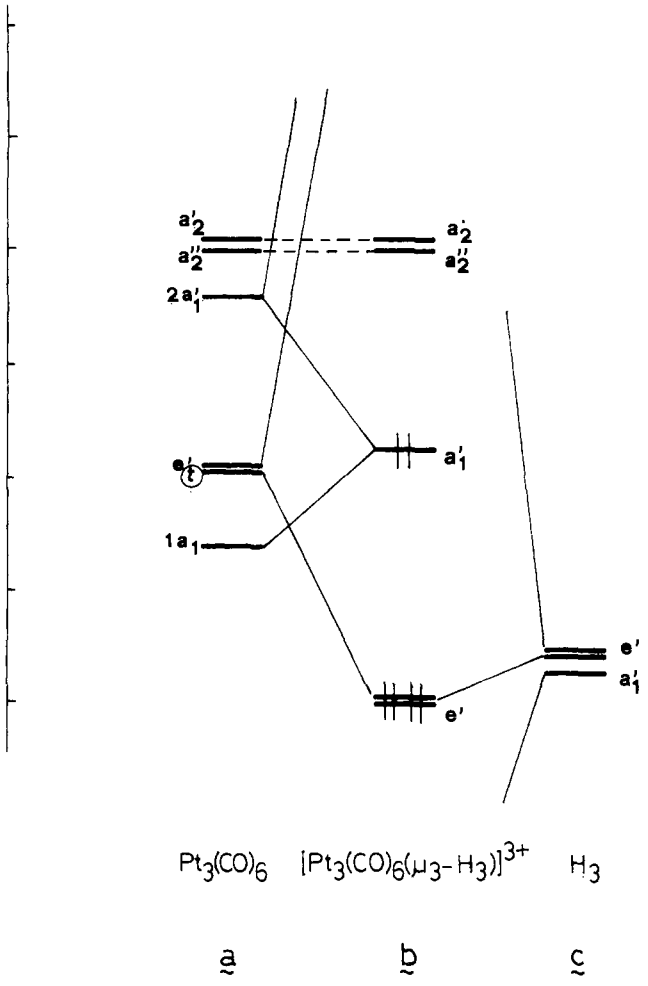

Figure 5. Diagram for the interaction between the FMOs of $Pt_3(CO)_6$ having geometry **7** and those of a H_3 grouping.

In summary, for all of the "supported-unbridged" examples the group(s) supporting the L_6M_3 skeleton operates to change the nature of the a'_1 radial bonding combination of the metals by rehybridizing and stabilizing it through a second-order effect. Through this action the metal $2a'_1$ level definitely stabilizes below the a'_2 level. It should be recalled that the relative order of these two levels, for naked L_6M_3 skeletons, is a function of the implosion parameter r (or the side of the equatorial triangle). The supporting coligands help to pass over an otherwise forbidden level crossing. Certainly it is not easy to assign the initial electron configurations of the interacting fragments. Somehow the coligand(s) provides the electrons necessary to fill the radial bonding combination of the metals which formally reach the d^{10} electron count. Hypothetically, if the coligand(s) could leave as a stable oxidized species (CO^{2+}, $SnCl_3^+$, or H^+), the reductive elimination of L_6M_3 could in principle be carried out.[29]

Finally, other examples of "supported-unbridged" L_6M_3 clusters, that are different by having the longest M–M distances, are found

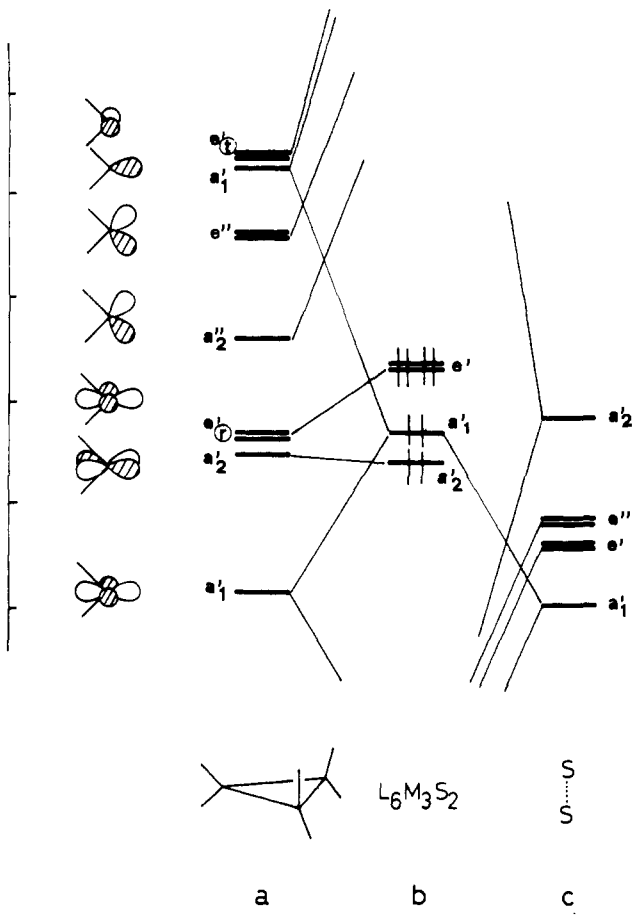

Figure 6. Interaction between the FMOs of a $Rh_3(CO)_6$ cluster having the longitudinal geometry **5** and those of two capping sulfur atoms. The L_2M orbitals used for building the different FMOs (a) are shown at the left of the figure.

in the compounds $[Rh_3(\mu^3\text{-}E)_2(CO)_6]^-$ (XII),[30] and $[Ni_3(\mu^3\text{-}E)_2(PEt_3)_6]^{2+}$ (XIII)[31] (E = S, Se). These are illustrated in **25**. There are two calcogenides that cap, on opposite faces, the M_3 triangle. The long M–M separations seem to suggest the absence of any metal–metal bonding. The three independent d^8 square-planar moieties are held together simply because the capping atoms function as cis ligands for each metal. Figure 6 shows an in-

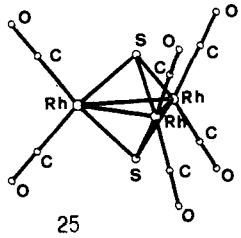

25

teraction diagram for a model of XII. The salient features are relative to the formation of six M–E bonds which originate from the interaction of the L_6M_3 skeleton, **5**, and the S_2 grouping. Three interactions concern the combinations of the well-known L_2M π hybrid. Since in this case the L_2M planes are orthogonal to the M_3 triangle the symmetries of these combinations are a''_2 and e''. The other M–S interactions which give rise to positive overlap populations (hence to three other M–S bonds) engage the empty in-plane orbitals e'_1 (formed by the metal p orbitals normal to the L_2M planes) and a'_1 (the radial combination of metal sp hybrids). Thus there remains little possibility for any direct metal–metal

(29) For a better understanding of the idea, think of the two limiting charges for the bridging H_3 grouping, namely H_3^{3-} and H_3^{3+}. In the former case each d^8 metal atom in XI and XII, described as square planarly coordinated by two terminal ligands and two bridging hydrides,[27] can hardly attain the stabilizing 16-e count. In fact the bridging hydrides cannot simultaneously donate two electron pairs to two adjacent metals. Also, the long M–M distances do not suggest that the closed-shell configuration is achieved by the d^{14} metal centers through the formation of M–M single bonds. According to the opposite viewpoint, the assembly of three d^{10} L_2M fragments, assisted by the presence of three protons, may be envisaged. As stated, the transfer of metal electrons to the protons weakens the M–M linkages. Obviously the actual situation is in between these extremes, but perhaps it is conceptually more useful to see the levels of Figure 5a populated up to $2a'_1$, as in this case three single M–M bonds would already be formed. The empty orbitals in Figure 5c have an overall stabilizing function, even though the partial transfer of the M–M bonding electrons to H_3^{3+} eventually lowers the M–M bond order.

(30) Galli, D.; Garlaschelli, L.; Ciani, G.; Fumagalli, A.; Martinengo, S.; Sironi, A. *J. Chem. Soc., Dalton Trans.* **1984**, 55–61.

(31) Cecconi, F.; Ghilardi, C. A.; Midollini, S. *Inorg. Chem.* **1983**, *22*, 3802–3808.

bonding mainly because there are no metal tangential orbitals which are opportunely split in filled bonding e'_1 and empty antibonding a'_2 combinations. On the other hand, there is some mixing of sp and x^2-y^2 character into the MO a'_1. But, at variance with many of the previous cases where mixing occurred with very little involvement of the ligand orbitals, here the level is largely M–S antibonding with the higher $2a'_1$ combination to avoid a greater destabilization. This is sufficient to prevent the M–M overlap population from vanishing. The calculated value has a small but not null value of 0.08.

Conclusions and Extensions

The correlations between stereochemistry, electron counts, nature of the ligands, M–M distances, etc., in skeletons of the type L_6M_3 are analyzed in some detail with the FMO method and perturbation theory arguments. In "unsupported-bridged" coordination the first-order interactions between the metal framework and the bridging ligands were found to be or primary importance in providing the necessary stability to the system. In addition, the origin of the M–M interactions occurring through second-order effects, such as a rehybridization of metal d–s–p orbitals, is clarified. Next the analysis of the "supported-unbridged" systems indicated that the most important cementing force within the M_3 triangle is the radial a'_1 bonding combination of the d–s–p metal hybrids. Tangential combinations of metal π orbitals help to strengthen the M–M linkages but do not seem mandatory for the existence of the triangular shape. In fact, the tangential combinations in some cases are used for the formation of linkages between the metals and the supporting ligands (see the case of the bridging H_3 group). In other cases (44-e complexes) they are populated even in their antibonding levels.

Hopefully these concepts, based on the selection of the MOs by symmetry and by their relative M–M or M–L bonding–antibonding character, may be extended to clusters of higher nuclearity.

Appendix

The extended Huckel calculations[32] utilized a modified version of the Wolfsberg-Helmoholz formula.[33] The parameters for C,O,H,S are standard ones,[32] those for Pt and Fe, Rh, Sn were taken from references 3b, 3i, 36 respectively. Unless otherwise specified the M–M distances are fixed at 2.70 Å in all calculations. The C–O distances used are 1.20 Å. In models **6** and **7** the cis (O)C-Pt-C(O) angles were 100°. In 16, the model of compound (7), the Fe-Pt and Fe-H distances are 2.60 and 1.60 Å respectively.

(32) Hoffmann, R.; Lipscomb, W. N. *J. Chem. Phys.* **1962**, *36*, 2179–2189, 3489–3493; **1962**, *37*, 2872. Hoffmann, R. *Ibid.* **1963**, *39*, 1397.
(33) Ammeter, J. H.; Burgi, H. B.; Thibeault, J. C.; Hoffmann, R. *J. Am. Chem. Soc.* **1978**, *100*, 3686–3692.
(34) Silvestre, J.; Albright, T. A.; Sosinsky, J. C. *Inorg. Chem.* **1981**, *20*, 3937–3940.

Theoretical Studies of the Polar Effect. 5.[1] The Use of the Isolated Molecule Approach

Stephen Marriott and Ronald D. Topsom*

Contribution from the Department of Chemistry, La Trobe University, Bundoora, Victoria, Australia 3083. *Received August 29, 1984*

Abstract: Substituent electronic effects on proton exchange reactions of various probes Y (Y = CO_2^-, NH_2, OH) according to the equation $XGYH^+ + HGY \rightleftharpoons XGY + HGYH^+$ have been shown to be closely approximated with isolated molecules instead of a molecular framework G. In particular, the equilibrium energies are well represented with use of calculations on the simple equilibrium $XH/HYH^+ + HH/HY \rightleftharpoons XH/HY + HH/HYH^+$. This latter equilibrium both allows a direct calculation of substituent field effects in systems of corresponding geometry and also provides a scale of σ_F values.

In recent years, the use of molecular orbital calculations has proved fruitful[2,3] in understanding the various modes of transmission of substituent electronic effects. Such calculations have also led to scales of inherent (that is, in the absence of solvent effects) substituent constants for field (σ_F),[4] electronegativity (σ_X),[5] and resonance effects (σ_F).[2,6] In both cases, considerable use has been made of, so called, isolated molecule calculations.

Calculations of isodesmic proton transfer reactions can be represented by the general reaction in eq 1, where X is a variable

$$XGYH^+ + HGY \rightleftharpoons XGY + HGYH^+ \qquad (1)$$

substituent, Y a probe group such as NH_2 or CO_2^-, and *G* a molecular framework. Experimental gas-phase energies for such processes where Y = NH_2 have been shown to be well reproduced by ab initio molecular orbital calculations (methylammonium,[7] quinuclidinium,[8] pyridinium, and anilinium ions[9]). Similar agreement has also been reported for substituted phenols[10] (Y = O^-).

Much recent interest[2,11,12] has concerned the relative importance of field and electronegativity effects. Experimental investigations here have mainly centered[13] on substituted quinuclidinium ions

(1) For Part 4 see ref 4.
(2) Topsom, R. D. *Acc. Chem. Res.* **1983**, *16*, 292.
(3) See, for example ref 4–10, 14–17, and the following: Wiberg, K. B. *J. Am. Chem. Soc.* **1980**, *102*, 1229. Vorpagel, E. R.; Streitweiser, A.; Alexandros, S. D. *J. Am. Chem. Soc.* **1981**, *103*, 3777. Pross, A.; Radom, L. *Prog. Phys. Org. Chem.* **1981**, *13*, 1. Reynolds, W. F.; Dais, P.; MacIntyre, D. W.; Topsom, R. D.; Marriott, S.; Von Nagy-Felsobuki, E.; Taft, R. W. *J. Am. Chem. Soc.* **1983**, *105*, 378. Marriott, S.; Topsom, R. D. *J. Chem. Soc., Perkin Trans. 2* **1984**, 113. Reynolds, W. F.; Mezey, P. G.; Hamer, G. K. *Can. J. Chem.* **1976**, *55*, 522.
(4) Marriott, S.; Topsom, R. D. *J. Am. Chem. Soc.* **1984**, *106*, 7.
(5) Marriott, S.; Reynolds, W. F.; Taft, R. W.; Topsom, R. D. *J. Org. Chem.* **1984**, *49*, 959.
(6) Marriott, S.; Topsom, R. D. *J. Chem. Soc., Perkin Trans. 2*, in press. Marriott, S.; Topsom, R. D. *J. Mol. Struct.* **1984**, *106*, 277.
(7) Taagepera, M.; Hehre, W. J.; Topsom, R. D.; Taft, R. W. *J. Am. Chem. Soc.* **1976**, *98*, 7438.
(8) Taagepera, M.; Taft, R. W.; Hehre, W. J.; Grob, C. A., unpublished results.
(9) Taagepera, M.; Summerhays, W. J.; Hehre, W. J.; Topsom, R. D.; Pross, A.; Radom, L.; Taft, R. W. *J. Org. Chem.* **1981**, *46*, 891.
(10) Pross, A.; Radom, L.; Taft, R. W. *J. Org. Chem.* **1980**, *45*, 818.
(11) Reynolds, W. F. *J. Chem. Soc., Perkin Trans. 2* **1980**, 985 and references therein.
(12) Exner, O. *Collect. Czech. Chem. Commun.* **1984**, *49*, 179 and references therein.
(13) See, for example: Charton, M. *Prog. Phys. Org. Chem.* **1981**, *13*, 119.

0002-7863/85/1507-2253$01.50/0